Passively Q-switched S-band thulium fluoride fiberlaser with multi-walled carbon nanotube

H. Ahmad* and S. A. Reduan

Photonics Research Centre, University of Malaya, Kuala Lumpur 50603, Malaysia
**Corresponding author: harith@um.edu.my*

Received October 7, 2017; accepted December 1, 2017; posted online January 2, 2018

A stable, passively Q-switched thulium fluoride fiber laser (TFFL) using a multi-walled carbon nanotube (MWCNT)-based saturable absorber (SA) for operation in the S-band region is proposed and demonstrated. The proposed TFFL has a central lasing wavelength of 1486.4 nm and an input power range of 87.1–126.6 mW. The output pulses have a repetition rate and pulse width range of 30.1–40.0 kHz and 9.0–3.2 μs, respectively, with a maximum pulse energy of 28.9 nJ. This is the first time, to the author's knowledge, of the successful demonstration of a passively Q-switched S-band TFFL using an MWCNT-based SA.

OCIS codes: 060.0060, 060.2430, 060.4370, 140.3510, 140.3540.
doi: 10.3788/COL201816.010609.

Recently, increased demands for information capacity and bandwidth have incurred significant limitations on existing communications infrastructure. Among the key reasons for this is the over-dependence on the C-band of optical fiber systems[1]. As such, substantial research efforts are now focused toward exploiting the L-band[2,3], 1.0 μm[4,5], and 2.0 μm[6,7] regions to increase bandwidth availability. Furthermore, recent developments have also seen the exploration of the S-band as a viable region for expanding the current communications bandwidth to cater to this increasing demand[1].

In communication systems particularly, pulsed sources operating at different bandwidths are crucial for the transmission of data. In this regard, Q-switched fiber lasers are highly desired for use in fiber laser systems due to their compact size, low fabrication, and operating cost as well as high flexibility[8,9]. Additionally, the output generated by these lasers have longer pulse widths and higher pulse energies, both of which are desired for communications applications[10], and finds significant applications in optical imaging, material processing, medicine, and environmental sensing[11–13].

Q-switching in fiber lasers can be realized through either active or passive means. Active Q-switching is achieved by modulating the output of the laser cavity using an external device, giving a high degree of control over various output parameters such the repetition rate and pulse width[14]. However, this technique requires complex electronics, significantly increasing the size and cost of the laser[15]. Passive Q-switching on the other hand offers less control over the output parameters, but is advantageous in terms of its compact form factor, low-cost, and flexibility of operation, thereby making them a preferred solution for many real-world operations[16].

One of the earliest means of generating passively Q-switched pulses was the use of semiconductor saturable absorber mirrors (SESAMs)[17,18]. While initially suitable for obtaining the desired output, its difficult integration into most fiber cavity designs, as well as limited bandwidth and high fabrication cost[19,20], spurred researchers to explore new means to generate passively Q-switched pulses. Research efforts thus begin to focus on saturable absorbers (SAs) and the discovery of 2D materials such as single-walled carbon nanotubes (SWCNTs) provided a significant breakthrough in the search for new SA materials[21,22]. This encouraged researchers to search for new SA-capable materials, including graphene[13,23] and more recently transition metal dichalcogenides (TMDs)[15], topological insulators (TIs)[24–26], and even exotic materials such as black phosphorus[27]. Recent advances have also seen the development of multi-walled carbon nanotubes (MWCNTs)[28] as SA materials, owing to their good thermal characteristics and higher mechanical strength as well as a better thermal stability and high photon absorption per nanotube efficiency due to the high multi-walls mass density[29]. This high density also affords MWCNTs a higher thermal damage threshold as the outer walls can protect the inner walls from damage or oxidation[29].

In this work, a passively Q-switched thulium-fluoride fiber laser (TFFL) operating in the S-band region and incorporating an MWCNT-based SA is proposed and demonstrated. To date, there have been only a few passively Q-switched fiber lasers in the S-band region reported, and even fewer that operate at the shorter wavelength range of the S-band region. It must be noted that while there have been previous works using erbium-doped fibers (EDFs)[2,24] and depressed-cladding EDFs (DC-EDFs)[30,31] as gain media in generating S-band pulsed laser outputs with the assistance of SAs, most of these lasers are only capable of partial S-band operation, and require the aid of tunable bandpass filters (TBPFs). In this work however, the combination of the thulium-fluoride fiber (TFF) as a gain medium and MWCNT-based SA has significant potential to generate passively Q-switched pulses in the S-band region, with the use of the TFF giving a large operational bandwidth from 1440 to 1500 nm.

This is crucial as it also covers the shorter wavelength region of the S band, which has eluded most efforts until today[32,33]. To the best of the author's knowledge, this work would be the first demonstrated use of an MWCNT-based SA in a TFFL cavity.

The MWCNT-based SA used in this experiment is prepared by homogenously dispersing the MWCNTs into a polyvinyl alcohol (PVA) host material. The preparation and fabrication processes employed in this work follows closely the method as outlined by Tiu *et al.*[34,35]. The characterization of the SA's nonlinear absorption is given in Fig. 1.

The Raman spectrum and the linear absorption of the MWCNT SA is also shown in Fig. 1 as insets (a) and (b) respectively. The twin-detector method is used to characterize the SA's nonlinear absorption using a homemade passively mode-locked EDF laser with a repetition rate and pulse width of 28.1 MHz and 0.73 ps respectively as a seed source. The collected data is fitted into the saturation model equation[36]

$$\alpha(I) = \frac{\alpha_s}{1 + I/I_{\text{sat}}} + \alpha_{\text{ns}}, \tag{1}$$

where $\alpha(I)$ is the intensity-dependent absorption, I is the pump light intensity, I_{sat} is the saturation intensity, α_s is the saturable loss (modulation depth) and α_{ns} is the non-saturable loss. From the fitted equation, the modulation depth and saturation intensity are measured to be 21.0% and 0.005 MW/cm^2 respectively. The modulation depth obtained is comparable to previous works using MWCNT-based SAs, such as that by Azooz *et al.*[20,37], who respectively obtained modulation depth values of 4% and 5.6%. The measured saturation intensity is also comparable to those in previous studies by Hassan[38], which reported a saturation intensity of around 0.18 MW/cm^2.

The Raman spectrum of the MWCNT SA shown in the inset of Fig. 1 was obtained using a Renishaw Raman spectroscope with a 1800 mm^{-1} grating and a 532 nm excitation wavelength. Four distinct peaks were observed, representing the D, G, G′, and D + G peaks at 1358, 1590, 2707, and 2903 cm^{-1}, respectively. These observed peaks can be compared to that obtained by Kasim *et al.*[4,29], and confirm the presence of MWCNTs. The G and G′ bands also indicate the presence of graphene and graphite as the MWCNT material consists of many graphene layers wrapped along the core tube[4]. The G band represents the in-plane tangential stretching of the carbon-carbon bonds on the nanotube wall plane[39], whereas the G′ band corresponds to the scattering of two phonons around the M and K points in the Brillouin zone[40]. The D bands indicates a multilayer configuration[4] and amorphous disordered carbon[34], thus proving that carbon nanotubes are in a multi-wall formation. Finally, the D + G band arises from the PVA host polymer of the SA[39].

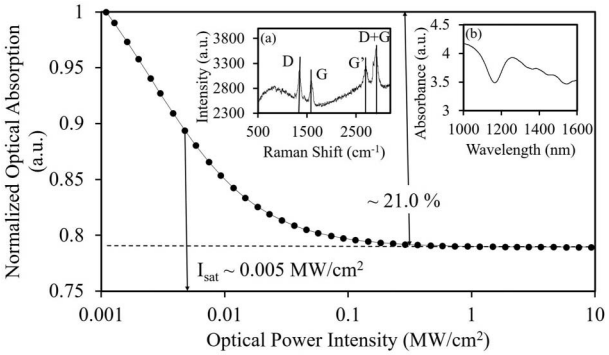

Fig. 1. Nonlinear absorption measurement of the MWCNT SA. Insets (a) The Raman spectrum and (b) the linear absorption of the SA.

The linear absorption of the MWCNT SA, as shown in inset (b) of Fig. 1, is obtained using a white light source ranging from 1000 to 1600 nm. It can be observed that the SA shows good absorbance of almost 4.2 a.u. at 1000 nm before reducing suddenly to 3.5 a.u. at 1168.0 nm. The absorbance then rises again to 2.73 a.u. at 1273.0 nm, and then reducing gradually again as it approaches 1600 nm. From these trends, the MWCNT-based SA can be seen to operate well in the S-band region.

The schematic diagram of the proposed passively Q-switched TFFL is shown in Fig. 2. The proposed laser consists of a 14.5 m long TFF from Fiberlabs Inc. as the gain medium, which has an absorption rate of 0.15 dB/m at 1400 nm as well as a numerical aperture of 0.26 and mode-field diameter of 4.5 μm at 1500 nm. The TFF is driven by a 1400 nm FOL1405RTD laser diode (LD) through an isolator and connected to the 1400 nm port of a 1400/1500 nm wavelength division multiplexer (WDM). The isolator serves to protect the LD from any damage that could arise from back reflections. The WDM's common port is connected to the TFF gain medium, with the other end of the TFF linked to a second isolator to ensure the unidirectional propagation of light within the proposed system. Immediately after the second isolator is a 90:10 optical coupler, which extracts 10% of the signal for further analysis. The remaining signal from the 90% port propagates through the cavity to reach the SA assembly, which is constructed by simply sandwiching a 2 mm by 2 mm portion of the aforementioned thin film

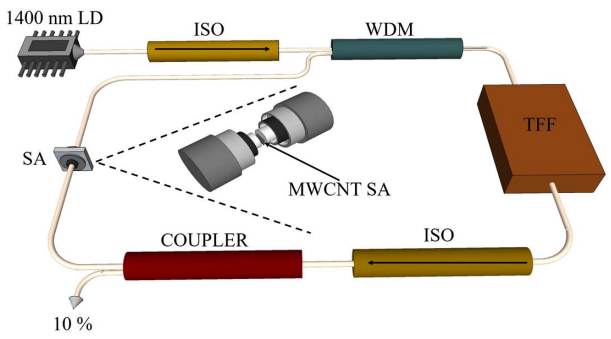

Fig. 2. Schematic diagram of a passive Q-switched TFFL.

MWCNT between two fiber ferrules with the aid of index matching gel and a fiber adaptor. The output of the SA is linked to the 1500 nm WDM port, thereby completing the optical circuit. The completed cavity has a total length of approximately 24.5 m.

The spectral characteristics of the generated pulses are analyzed using an Anritsu MS9740A optical spectrum analyzer (OSA), while its pulse characteristics are examined by a Yokogawa DLM2054 oscilloscope (OSC). An Anritsu MS2683 radio-frequency spectrum analyzer (RFSA) is used to observe the signal-to-noise ratio (SNR) of the corresponding radio frequency (RF) spectrum, and a Thorlabs PM100USB optical power meter (OPM) is used to monitor the output power of the laser.

The characteristics of the Q-switched output pulses at a pump power of 99.4 mW are shown in Fig. 3. The optical spectrum of the Q-switched pulses is given in Fig. 3(a), with a central wavelength of 1486.4 nm and a 3 dB spectral width of approximately 0.8 nm. The corresponding pulse train of the Q-switching operation as shown in inset (a) of Fig. 3(a) has a repetition rate of 32.1 kHz and pulse width or full width at half-maximum (FWHM) of 4.6 μs. There are minimal intensity instabilities and minimal pulse-to-pulse timing jitter of the generated pulses, as shown in inset (b) of Fig. 3(a). The RF spectrum of the Q-switched pulses at the same pump power are given in Fig. 3(b). From the figure, an SNR value of around 50.0 dB at the fundamental frequency, $f_0 = 32.1$ kHz, can be obtained. The high SNR value indicates substantially stable Q-switched pulses, comparable to those obtained in other works using different SAs[15]. Insets (a) and (b) of Fig. 3(b) provide a wideband RF spectrum and the stability of the Q-switching operation.

Figure 4(a) shows the repetition rate and pulse width trends of the Q-switched pulses against an increasing pump power range of 87.1–126.6 mW. It can be seen from the figure that the repetition rate increases almost linearly from 30.1 to 40.0 kHz as the pump power rises toward the maximum pump power of 126.6 mW, and this trend is a typical characteristic of Q-switched pulses[13,30,41]. Crucially, the rising repetition rate is indicative that the system is not mode locked, in which case the repetition rate of the pulses remains unchanged even as the pump power rises[42]. Furthermore, the pulse width decreases exponentially over the same pump power range, narrowing from 9.0 to 4.2 μs as the pump power rises from 87.1 to 101.6 mW, as would be expected from a Q-switched system. Further increases in the pump power now leads to a more linear narrowing of the pulse width, from 4.0 μs at a pump power of 103.8 mW to 3.3 μs at a pump power of 118.3 mW before finally plateauing out at 3.2 μs until the maximum pump power is reached. This is attributed to the SA reaching saturation[15,43].

The average output power and pulse energy response to the rising pump power is given in Fig. 4(b). Both trends increase linearly with the rising pump power, with a maximum average output power and pulse energy of 1.2 mW and 28.9 nJ, respectively, obtained at the maximum pump

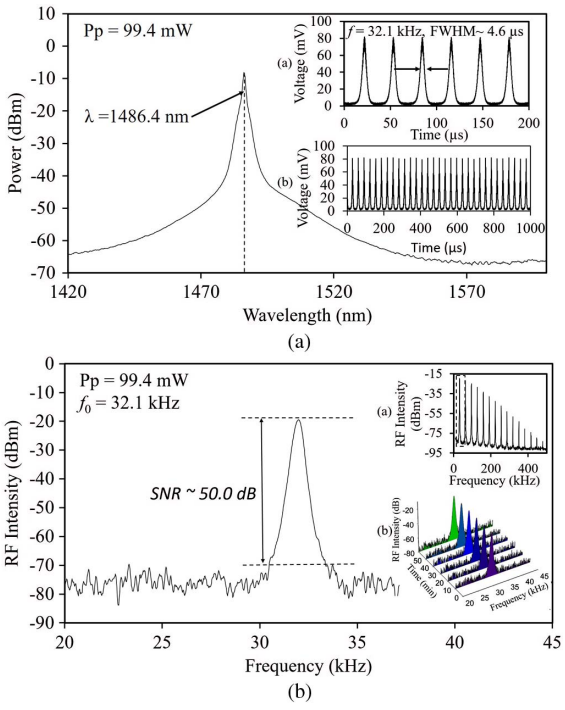

Fig. 3. Characteristics of Q-switched output pulses at a pump power of 99.4 mW. (a) The optical spectrum ($\lambda = 1486.4$ nm) and pulse train of the Q-switching operation [inset (a) and (b)] and (b) the RF spectrum at the fundamental frequency ($f_0 = 32.1$ kHz) wideband RFSA spectrum [inset (a)] and stability of the Q-switching operation for 1 h [inset (b)].

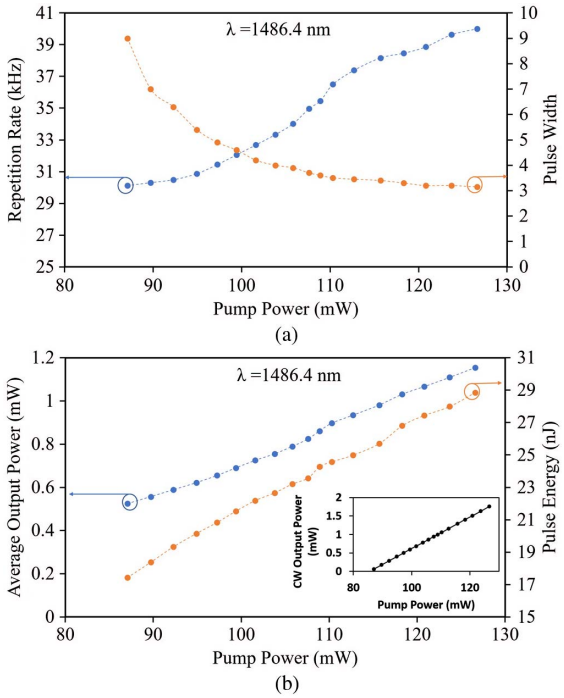

Fig. 4. (Color online) Trends of (a) the repetition rate and pulse width and (b) the average output power and pulse energy against the increasing pump power and the CW output power as a function of pump power (inset).

Table 1. Characteristics of Passive Q-switched Pulse Output of S-band Fiber Laser

Type of SA	Wavelength (nm)	Repetition Rate (kHz)	Min. Pulse Width (μs)	Max. Pulse Energy	Ref.
Graphene	1512.0	14.6–55.3	1.6	25.8 nJ	[44]
TI: Bi_2Te_3	1510.9	2.15–12.8	13	1.525 μJ	[24]
$MoSe_2$	1491.6	34.5–90.0	1.0	2.3 nJ	[45]
MWCNT	1486.4	30.1–40.0	3.2	28.9 nJ	This work

power $P_{max} = 126.6$ mW. It is noted that above P_{max}, Q-switched pulses can no longer be observed. Furthermore, the various parameters of the pulses become unstable before Q-switching ceases, indicating that the SA has become fully saturated. However, reducing the pump power to below P_{max} results in the pulses reappearing. This is an important observation as it confirms that the SA has not experienced thermal damage.

Most Q-switched S-band fiber laser designs commonly utilize EDFs or DC-EDFs as the primary gain media, with TBPFs used to confine the central lasing wavelength to within the S-band region[24,44,45]. However, the need for the TBPF induces a loss in the system, thereby reducing the overall performance of the Q-switched laser. In this work, the use of the TFF as the gain medium in combination with the MWCNT-based SA allows for laser pulses to be realized in the S-band region without the need for a TBPF. The performance of the proposed laser in this work, compared to other SA-based S-band Q-switched lasers is given in Table 1. From the table, it can be seen that the proposed laser in this work is capable of operating in the shortest wavelength range of the S-band region in comparison to other works[24,44,45], with the added advantage of not requiring a TBPF in the cavity.

While other works successfully demonstrates Q-switched pulses with smaller pulse widths of 1.6 μs and 1.0 μs, such as those by Muhammad *et al.*[44] and Ahmad *et al.*[45], the pulses produced in this work have the advantage of having a higher pulse energy. In a similar manner, other works such as that by Chen *et al.*[24] are capable of generating pulses with higher energies; these pulses have wider pulse widths and a narrower repetition rate range as compared to the pulses generated by the proposed system of this work[44,45]. It is also possible to obtain a pulsed laser output at shorter S-band wavelengths and larger single-pulse energy, utilizing the same gain medium but different SA[46], although at the price of a slightly wider pulse width and lower maximum repetition rate. Overall, Q-switched outputs with higher pulse energies and shorter pulse widths are desired for photonics applications, particularly in the S-band region[16]. Thus, the proposed laser of this work has significant potential for the generation of passive Q-switched pulses in the S-band region, particularly in the shorter S-band wavelengths, giving it a high potential for realizing multiple photonic applications.

In conclusion, the passively Q-switched S-band TFFL using an MWCNT-based SA is successfully proposed and demonstrated. A 14.5 m long TFF is used as a gain medium, whereas a thin film MWCNT is used as an SA to generate the desired Q-switched pulses. The proposed laser has a central lasing wavelength of 1486.4 nm, and generates stable output pulses with a repetition rate from 30.1 to 40.0 kHz and a pulse width from 9.0 to 3.2 μs over a pump power range of 87.1–126.6 mW. The maximum average pump power and pulse energy observed are 1.2 mW and 28.9 nJ, respectively. The stability of the pulsed laser is verified by an SNR of 50.0 dB, obtained from its corresponding RFSA spectrum. This makes the proposed laser highly advantageous for generating Q-switched pulses in the S-band region, especially the shorter wavelength of the S-band, without the need for a TBPF.

We would like to acknowledge the Ministry of Higher Education, Malaysia for funding for this work under Grant No. LRGS (2015) NGOD/UM/KPT and the University of Malaya for funding for this work under Grant Nos. RP 029 A - 15AFR and RU 001 - 2017.

References

1. L.-G. Yang, S.-S. Jyu, C.-W. Chow, C.-H. Yeh, and Y. Lai, Laser Phys. Lett. **11**, 015105 (2013).
2. B. Dong, J. Hu, C.-Y. Liaw, J. Hao, and C. Yu, Appl. Opt. **50**, 1442 (2011).
3. S. J. Tan, S. W. Harun, H. Arof, and H. Ahmad, Chin. Opt. Lett. **11**, 073201 (2013).
4. N. Kasim, A. Al-Masoodi, F. Ahmad, Y. Munajat, H. Ahmad, and S. Harun, Chin. Opt. Lett. **12**, 031403 (2014).
5. J. Du, Q. Wang, G. Jiang, C. Xu, C. Zhao, Y. Xiang, Y. Chen, S. Wen, and H. Zhang, Sci. Rep. **4**, 6346 (2014).
6. H. Ahmad, A. Muhamad, A. Sharbirin, M. Samion, and M. Ismail, Opt. Commun. **383**, 359 (2017).
7. Z. Chu, J. Liu, Z. Guo, and H. Zhang, Opt. Mater. Express **6**, 2374 (2016).
8. S. Orazio, *Principles of Lasers* (Springer, 2010).
9. A. Denisov, A. Kuznetsov, D. Kharenko, S. Kablukov, and S. Babin, Laser Phys. **21**, 277 (2011).
10. O. Svelto, *Principles of Lasers* (Springer, 2010).
11. U. Sharma, C.-S. Kim, J. U. Kang, and N. M. Fried, in *Laser Applications to Chemical and Environmental Analysis* (2004), paper MB3.
12. M. L. Siniaeva, M. N. Siniavsky, V. P. Pashinin, A. A. Mamedov, V. I. Konov, and V. V. Kononenko, Laser Phys. **19**, 1056 (2009).
13. D. Popa, Z. Sun, T. Hasan, F. Torrisi, F. Wang, and A. Ferrari, Appl. Phys. Lett. **98**, 073106 (2011).

14. M. Delgado-Pinar, D. Zalvidea, A. Diez, P. Pérez-Millán, and M. Andrés, Opt. Express **14**, 1106 (2006).
15. B. Chen, X. Zhang, K. Wu, H. Wang, J. Wang, and J. Chen, Opt. Express **23**, 26723 (2015).
16. T. Y. Tsai and Y. C. Fang, Opt. Express **17**, 1429 (2009).
17. X. Yin, J. Meng, J. Zu, and W. Chen, Chin. Opt. Lett. **11**, 081402 (2013).
18. R. Paschotta, R. Häring, E. Gini, H. Melchior, U. Keller, H. Offerhaus, and D. Richardson, Opt. Lett. **24**, 388 (1999).
19. L. Zhang, Y. Wang, H. Yu, L. Sun, W. Hou, X. Lin, and J. Li, Laser Phys. **21**, 1382 (2011).
20. S. Azooz, F. Ahmad, H. Ahmad, S. Harun, B. Hamida, S. Khan, A. Halder, M. C. Paul, M. Pal, and S. K. Bhadra, Chin. Opt. Lett. **13**, 030602 (2015).
21. D.-P. Zhou, L. Wei, B. Dong, and W.-K. Liu, IEEE Photon. Technol. Lett. **22**, 9 (2010).
22. H. Ma, Y. Wang, W. Zhou, J. Long, D. Shen, and Y. Wang, Laser Phys. **23**, 035109 (2013).
23. Z. Luo, M. Zhou, J. Weng, G. Huang, H. Xu, C. Ye, and Z. Cai, Opt. Lett. **35**, 3709 (2010).
24. Y. Chen, C. Zhao, S. Chen, J. Du, P. Tang, G. Jiang, H. Zhang, S. Wen, and D. Tang, IEEE J. Sel. Top. Quantum Electron. **20**, 315 (2014).
25. Y. Chen, C. Zhao, H. Huang, S. Chen, P. Tang, Z. Wang, S. Lu, H. Zhang, S. Wen, and D. Tang, J. Lightwave Technol. **31**, 2857 (2013).
26. P. Tang, X. Zhang, C. Zhao, Y. Wang, H. Zhang, D. Shen, S. Wen, D. Tang, and D. Fan, IEEE Photon. J. **5**, 1500707 (2013).
27. Y. Chen, G. Jiang, S. Chen, Z. Guo, X. Yu, C. Zhao, H. Zhang, Q. Bao, S. Wen, and D. Tang, Opt. Express **23**, 12823 (2015).
28. H. Yu, L. Zhang, Y. Wang, S. Yan, W. Sun, J. Li, Y. Tsang, and X. Lin, Opt. Commun. **306**, 128 (2013).
29. F. Ahmad, H. Haris, R. Nor, N. Zulkepely, H. Ahmad, and S. Harun, Chin. Phys. Lett. **31**, 034204 (2014).
30. H. Ahmad, M. Soltanian, L. Narimani, I. Amiri, A. Khodaei, and S. Harun, IEEE Photon. J. **7**, 1 (2015).
31. H. Ahmad, M. A. Ismail, M. Suthaskumar, Z. C. Tiu, S. W. Harun, M. Z. Zulkifli, S. Samikannu, and S. Sivaraj, Laser Phys. Lett. **13**, 035103 (2016).
32. R. Caspary, U. B. Unrau, and W. Kowalsky, in *Proceedings of 2003 5th International Conference on Transparent Optical Networks* (2003), p. 236.
33. S. Tanabe and T. Tamaoka, J. Non-Cryst. Solids **326**, 283 (2003).
34. Z. C. Tiu, F. Ahmad, S. J. Tan, A. Zarei, H. Ahmad, and S. W. Harun, J. Mod. Opt. **61**, 1133 (2014).
35. H. Ahmad, M. Ismail, S. Hassan, F. Ahmad, M. Zulkifli, and S. Harun, Appl. Opt. **53**, 7025 (2014).
36. R. Woodward, E. Kelleher, R. Howe, G. Hu, F. Torrisi, T. Hasan, S. Popov, and J. Taylor, Opt. Express **22**, 31113 (2014).
37. H. Ahmad, S. Hassan, F. Ahmad, M. Zulkifli, and S. Harun, Opt. Commun. **365**, 54 (2016).
38. S. N. M. Hassan, *Multiwall Carbon Nanotube (MWCNT) as a Saturable Absorber for Generation of High Q-factor in Erbium Doped Fiber Laser (EDFL)* (Institut Pengajian Siswazah, Universiti Malaya, 2016).
39. J. Kürti, V. Zólyomi, A. Grüneis, and H. Kuzmany, Phys. Rev. B **65**, 165433 (2002).
40. N. Chakrapani, S. Curran, B. Wei, P. M. Ajayan, A. Carrillo, and R. S. Kane, J. Mater. Res. **18**, 2515 (2003).
41. H. Ahmad, S. Reduan, S. Aidit, and Z. Tiu, Chin. Opt. Lett. **15**, 020601 (2017).
42. D. Mao, X. Liu, and H. Lu, Opt. Lett. **37**, 2619 (2012).
43. N. Aziz, A. Latiff, M. Lokman, E. Hanafi, and S. Harun, Chin. Phys. Lett. **34**, 044202 (2017).
44. F. Muhammad, M. Zulkifli, and H. Ahmad, J. Nonlinear Opt. Phys. Mater. **23**, 1450004 (2014).
45. H. Ahmad, M. Ismail, S. Sathiyan, S. Reduan, N. Ruslan, C. Lee, M. Zulkifli, K. Thambiratnam, M. Ismail, and S. Harun, Opt. Commun. **382**, 93 (2017).
46. H. Ahmad, S. Reduan, A. Zulkifli, and Z. Tiu, Appl. Opt. **56**, 3841 (2017).